



encit 2020



18th Brazilian Congress of Thermal Sciences and Engineering
November 16-20, 2020 (Online)

ENC-2020-0761

USE OF BRAZILIAN SOLAR EXPERIMENTAL DATA TO ASSESS DISH/STIRLING TECHNOLOGY

Oscar R. Sandoval

Centro Universitário UNA – Contagem.

e-mail: oscar.rodriguez@prof.una.br

Vitor Mourão Hanriot

Bryan Castro Caetano

Universidade Federal de Minas Gerais, Colegiado de graduação em Controle e Automação

e-mails: oscar.rodriguez@prof.una.br; vmouraoh@hotmail.com

Juan José García Pabón

Diego Mauricio Yepes Maya

Federal University of Itajubá – UNIFEI

e-mails: jjgp@unifei.edu.br; diegoyepes@unifei.edu.br

Keywords: solar radiation, beam radiation, parabolic dish, Stirling, solar energy

1. INTRODUCTION

Access to quality electrical energy is a priority for the continuous development of a country, however, this access is commonly hampered by its territorial size, especially in Brazil, which due to having an area of approximately 8.5 million km² makes transmission difficult and the distribution of this energy (Xavier et al., 2015). For this reason, distributed generation has the main function of bringing energy to sectors far from large urban centers and encouraging human development in isolated areas. For this, technological advances must be accompanied by the development of systems that allow this type of generation (Prinsloo, Dobson and Mammoli, 2016).

To reduce the consumption of petroleum-based fuels and, consequently, the emission of polluting and greenhouse gases, several technologies are being studied to increasingly take advantage of the available renewable resources, in which solar energy is one of the most important sources. Attractive in Brazil due to wide daily availability. Solar energy can be transformed into electrical, thermal, and mechanical energy using various technologies, such as photovoltaic panels (do Nascimento et al., 2020; Xavier et al., 2015), solar collectors (Cruz et al., 2020; Devabhaktuni et al., 2013) and parabolic concentrating dishes with Stirling engines (Sandoval et al., 2019; Mendoza Castellanos et al., 2017). According to Devabhaktuni et al. (Devabhaktuni et al., 2013), photovoltaic panels are semiconductor devices that convert solar energy, concentrated and non-concentrated, into electrical energy. Solar collectors, flat plate, and vacuum tubes transform the non-concentrated energy contained in the sun's rays into thermal energy for heating or cooling purposes. In Brazil, this technology is widely used for heating water (Sandoval, Koury and Maia, 2016). Parabolic concentrating discs are associated with Stirling engine technology. The parabolic dish concentrates the sun's rays at a focal point where the Stirling engine receives the energy in the form of heat and transforms it into mechanical power or electrical energy using a generator.

Among the technologies for harnessing solar energy, the parabolic concentrating dish with Stirling engine is the least widespread technology in Brazil, leading the scientific community to carry out studies to better understand the functioning and the gains obtained with the implementation (Mendoza Castellanos et al., 2017), mainly in a country with the privilege of the amount of available daily solar radiation, which is even higher than in countries where the use of this technology is widespread. Thus, to study the behavior of solar technologies, mathematical models and solar data collected on the ground are used to quantify, together with the mathematical model of the technology to be studied, the transformation of solar energy into useful energy in the national energy scenario (Sandoval et al., 2019; Mendoza Castellanos et al., 2017). For this reason, this work presents, based on the use of an experimental solar base, a solar forecast model, and a model for predicting the characteristics of a parabolic concentrating dish with Stirling engine technology, the evaluation is made in Brazilian regions. For this, the global radiation data measured on the ground are statistically treated and used to determine the output shaft power as a function of the direct radiation reaching the concentrating dish in each of the regions

2. EXPERIMENTAL SOLAR BASE AND SOLAR FORECAST MODEL

2.1 Experimental Solar Base

The horizontal global solar radiation data are obtained from the database of the National Organization of Environmental Data System - SONDA (<http://sonda.ccst.inpe.br/>) for the eight stations shown in Tab. 1. The choice of solar stations is due to the positioning in the national territory, as the data collected between the years 2009 and 2018 are treated to determine global solar radiation in the horizontal characteristic for the northeast, southeast and south regions.

To reduce computational time and present a methodology for evaluating solar technology, a statistical treatment of the collected data is performed to quantify the monthly hourly averages of the months that comprise the summer season in the southern hemisphere, that is, for December, January, February, and March.

Table 1 - Specifications of the REDE SONDA acquisition stations.

ZONE	CODE	ESTATION	LATITUD	LONGITUD	YEAR			
Northeast	NAT	Natal	05°50'12''S	35°12'23''O	2011	2015	2016	
	PTR	Petrolina	09°04'08''S	40°19'11''O	2014	2015	2016	
	SLZ	São Luiz	02°35'36''S	44°12'44''O	2014	2015	2016	
Southeast	CPA	Cachoeira Paulista	22°41'23''S	45°00'22''O	2015	2016	2017	2018
	ORN	Ourinhos	22°56'55''S	49°53'39''O	2009		2010	
South	JOI	Joinville	26°15'09''S	26°15'09''S	2012	2013	2014	
	SBR	Sombrio	29°05'44''S	29°05'44''S	2013	2014	2015	
	SMS	São Martinho da Serra	29°26'34''S	53°49'23''O	2009	2011	2012	2013

Fig. 1 shows the average hourly global solar radiation data for each of the evaluated solar stations. Although they are located in the same geographic region, it is observed that for the same region and month, the daily data show variations in radiation intensity. This is observed for the month of December in the Northeast region, in which the SLZ station in the year 2016 has a maximum average monthly radiation of 604 W / m^2 , while the NAT and PTR stations for the same year, 869.8 W / m^2 and 888.6 W / m^2 , respectively.

Due to variations in intensities and in order to better represent the three regions analyzed, for each region and in each month the global hourly average solar radiation is determined, which allows the evaluation of solar technology using the average data that represent the intensity obtained in the locality. In this analysis, and as shown in Fig. 1, the NAT solar station in March 2011, as well as the CPA solar station in February 2017, present corrupted hourly average data, being removed in the hourly average for the evaluated month.

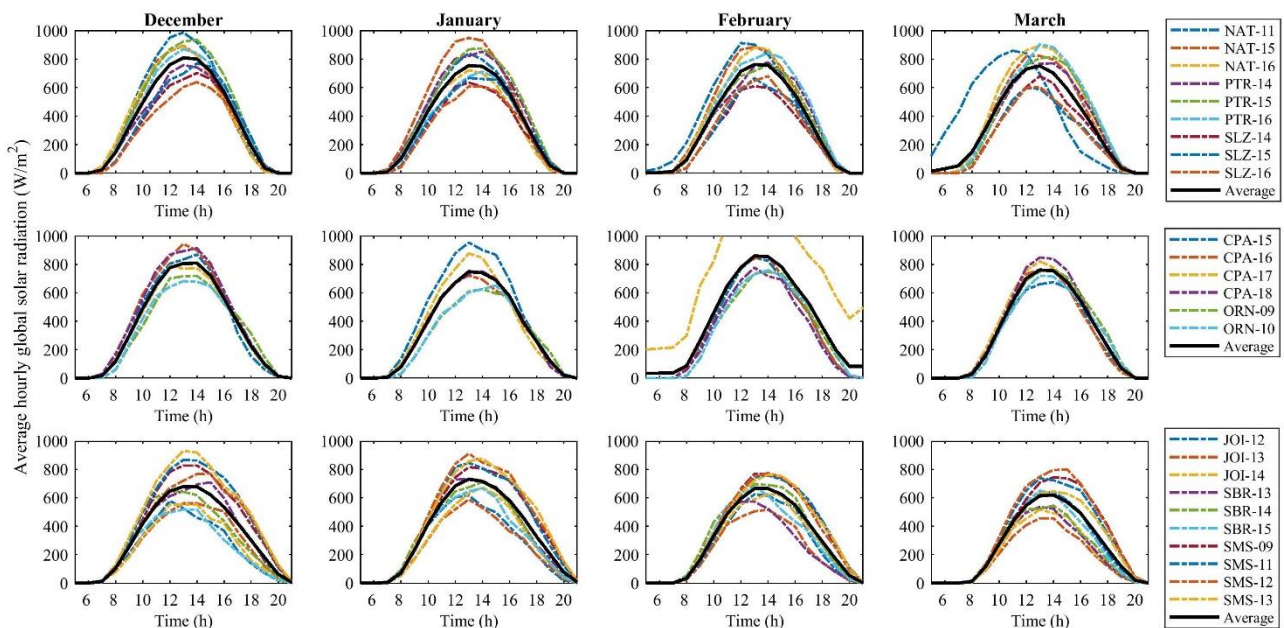


Figure. 1 - Horizontal global solar radiation curves for the evaluated stations.

Based on the average behavior of the global average hourly monthly radiation horizontally for the northeast, southeast, and south regions, a solar forecasting model is used to identify the portion of direct radiation that the concentrating dish, which uses a solar tracking system, receives over the standard day for each month. These data are used to evaluate the power generation Stirling cycle.

2.2. Solar forecasting model

According to Duffie and Beckman (2013), solar radiation reaching any object on the earth's surface is found in three components, which are called direct radiation, diffuse radiation, and reflected radiation. Parabolic concentrating discs usually work with a two-axis tracking system, that is, direct radiation is used in the plane of the concentrating disc (I_{bT}), which is calculated using Eq. (1).

$$I_{bT} = I_b R_b \quad (1)$$

Where direct radiation in the horizontal plane (I_b) and the relationship between direct radiation in the plane and horizontal (R_b) is determined by Eq. (2) and (3), respectively.

$$I_b = I - I_d \quad (2)$$

$$R_b = \frac{\cos(\varphi - \theta_Z) \cos(\delta) \cos(\omega) + \sin(\varphi - \theta_Z) \sin(\delta)}{\cos(\varphi) \cos(\delta) \cos(\omega) + \sin(\varphi) \sin(\delta)} \quad (3)$$

In Eq. (2), variable I indicate the total horizontal radiation measured experimentally, which is obtained from the database presented in section 2.1. I_d is the diffuse horizontal radiation described in Eq. 4 obtained by the solar forecast model. In Eq. (3), the variable ϕ indicates the latitude of the evaluated location. In this work, three average latitudes are used, one for each region, determined with the data presented in Tab. 1. The variable θ_Z indicates the zenith angle at the time of assessment, δ indicates the daily declination, and ω the average hourly solar angle

$$\frac{I_d}{I} = \begin{cases} 1.0 - 0.09k_T & \text{para } k_T \leq 0.22 \\ 0.9511 - 0.164k_T + 4.388k_T^2 - 16.638k_T^3 + 12.336k_T^4 & \text{para } 0.22 < k_T \leq 0.80 \\ 0.165 & \text{para } k_T > 0.8 \end{cases} \quad (4)$$

In Eq. (4) the term k_T is known as the lightness index in the evaluated location. This index is obtained from the relation presented in Eq. (5), in which the term I_o is the extraterrestrial hourly radiation defined by Eq. (6).

$$k_T = \frac{I}{I_o} \quad (5)$$

$$I_o = \frac{12G_{sc}}{\pi} \left(1 + 0.033 \cos\left(\frac{360n}{365}\right) \right) \times \left[\cos(\varphi) \cos(\delta) \left(\sin(\omega_1) - \sin(\omega_2) + \frac{\pi(\omega_2 - \omega_1)}{180} \right) \text{sen}(\varphi) \text{sen}(\delta) \right] \quad (5)$$

Where G_{sc} is the solar constant equal to 1367 W / m², ω_1 and ω_2 are the limits of the evaluated time range.

Finally, θ_Z and δ are determined using Eq. (6) and (7), knowing that the average solar days (n) of December, January, February, and March are 344, 17, 47, and 75, respectively.

$$\theta_Z = \cos^{-1}(\cos(\varphi) \cos(\delta) \cos(\omega) + \cos(\varphi) \cos(\delta)) \quad (6)$$

$$\delta = 23.45^\circ \text{sen}\left(360 \frac{284+n}{365}\right) \quad (7)$$

The solar forecasting model is used to determine, from the data collected experimentally, the component of direct solar radiation in the plane of the concentrating parabolic dish.

3. CONCENTRATOR DISC AND STIRLING MOTOR MODEL

As described in the work by Sandoval et al. (2019), the evaluation model of a parabolic concentrating disc working in conjunction with a Stirling engine follows the steps shown in Fig. 2. After determining the direct radiation in the plane of the parabolic disc, the prediction of the concentrated power is determined for a 7.5 m

concentrating dish. Finally, with concentrated power, the Stirling power axis prediction model predicts engine operation.

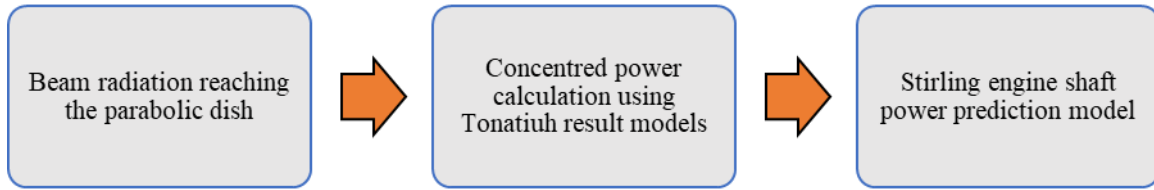


Figure 2 – Step of analysis for solar technology.

3.1. Parabolic dish power prediction model

The concentrating dish used is shown in Fig. 3. The operation of a parabolic concentrating dish using a Stirling engine is simple since the direct solar radiation that is collected by the dish is concentrated in a focal point called the focus. In this focus, the hot chamber of the Stirling engine is positioned, so a portion of the heat concentrated by the disc is used as heat input for the Stirling cycle, transforming it into mechanical shaft work.

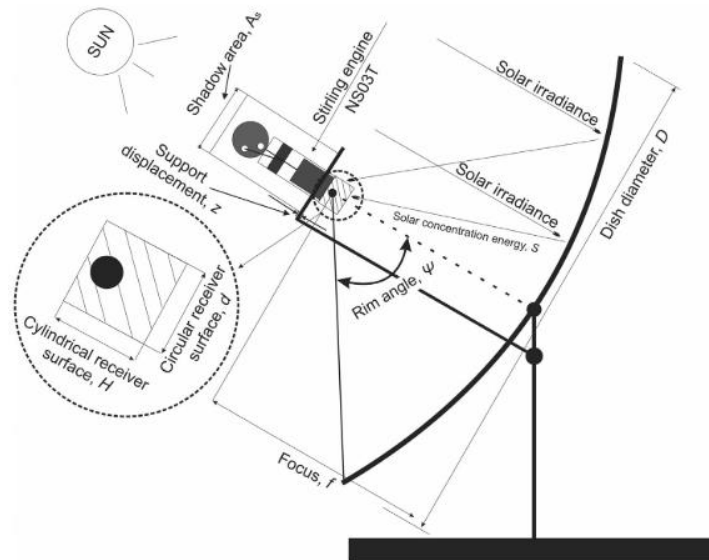


Fig. 3 – Concentrating disc using a Stirling engine (Sandoval et al., 2019).

The concentrating dish is simulated in the Tonatiuh program using the geometry and material shown in Tab. 2. As a result of the program, Eq. (8) and (9) describe the concentrated dish forecasting model of the concentrating dish. Eq. (8) describes the power received in the cylinder of the Stirling engine and Eq. (9) in the front circle. These two regions are illustrated in Fig. 3. According to Sandoval et al. (2019), the sum of these two powers is the power available at the Stirling engine receiver.

Table 2 – parabolic solar dish concentrator (Sandoval et al., 2019).

Parameter	Value
Receiver diameter	0.07 m
Receiver height	0.0835 m
Receiver thickness	0.001 m
Diameter of parabolic dish	7.5 m
Shadow surface by Stirling	0.1627 m ²
f/D	0.65
Material receptor	Steel inox 304
CRS	0.02
Mirror reflectance	0.94
Number of photons in the simulation	10×10 ⁷

$$P_{cil} = 15.4070I_{bt} - 0.0554 \quad (8)$$

$$P_{cir} = 14.2310I_{bt} - 0.1921 \quad (9)$$

3.2. Stirling engine shaft power prediction model

This work uses the modified Iwamoto model described by Sandoval et al. (Sandoval et al., 2019), which calculates the output shaft power of the Stirling engine based on dimensionless numbers formulated from the experimental characteristics of 26 Stirling search and commercial engines. The modified Iwamoto model is formulated from Eq. (10) to (17). Thus, the first step is to determine the dimensionless pressure (P^*), temperature (T^*), and engine speed (n^*) using Eq. (10) to (12). The second step is to calculate the dimensionless specification (S^*) using Eq. (14). Therefore, the last step is to determine the dimensionless output power (L^*) and the dimensionless work (W_S^*) using Eq. (15) and (16), respectively.

$$P^* = \frac{P_m}{P_{tim}} \quad (10)$$

$$T^* = \frac{T_H - T_C}{T_H + T_C} \quad (11)$$

$$n^* = 3 \times 10^{-6} S^{*0.6855} \quad (12)$$

$$S^* = \frac{T_H R V_{SE}^{2/3}}{v^2} \quad (13)$$

$$L^* = 0.0262 n^{*1.1982} \quad (14)$$

$$W_S^* = \frac{W_S}{P_m V_{SE} P^* T^*} \quad (15)$$

Where W_S is the number of West defined by Eq. (16) and v is the kinetic viscosity of the fluid at hot temperature (T_H) and average pressure (P_m), is defined by Eq. (17). According to Sripakagorn and Srikam (2011), the West number for a Stirling engine with power below 5 kW is 0.35. Parameters of the NS03T Stirling engine used in this work are presented in the Tab. 3.

$$W_S = \frac{L_S}{P_m V_{SE} n T^*} \quad (16)$$

$$v = \frac{Pr_{ar} R T_H^{(1+\mu_b)}}{P_m} \quad (17)$$

Table 3 – Specifications of NS03T Stirling and work fluid (Sandoval et al., 2019).

Parameter	Value
Volume dislocated, V_{SE}	192 cm ³
Working fluid	Helium
Mean pressure, P_m	6.1 MPa
Hot chamber temperature, T_H	Variable with radiation
Engine rotation	500-1500 rpm
Cold chamber temperature, T_C	298 K
Maximum power output	>3 kW
Maximum thermal efficiency	32%
Gas constant, R	2077.1 J/(kg K)
Prandtl number, Pr	0.6981
Dynamic viscosity, μ_b	3.709×10^{-7} Pa s

4. RESULTS AND DISCUSSION

Using the experimental data and the forecast model of solar characteristics, Fig. 4 shows the average monthly direct radiation in the plane of the parabolic dish. As noted, the region with the highest intensity is the Southeast region, on the other hand, the Northeast region has a medium behavior, and the South region the least intense when the months of December and March are observed. In January, the southern and southeastern regions present the best direct solar radiation to the parabolic concentrating dish, this is a consequence of the latitudes of the south and southeast regions. Finally, the equinox in March identifies the low direct radiation collected by the parabolic disc in the south of the country, reaching maximum levels of 300 W/m^2 .

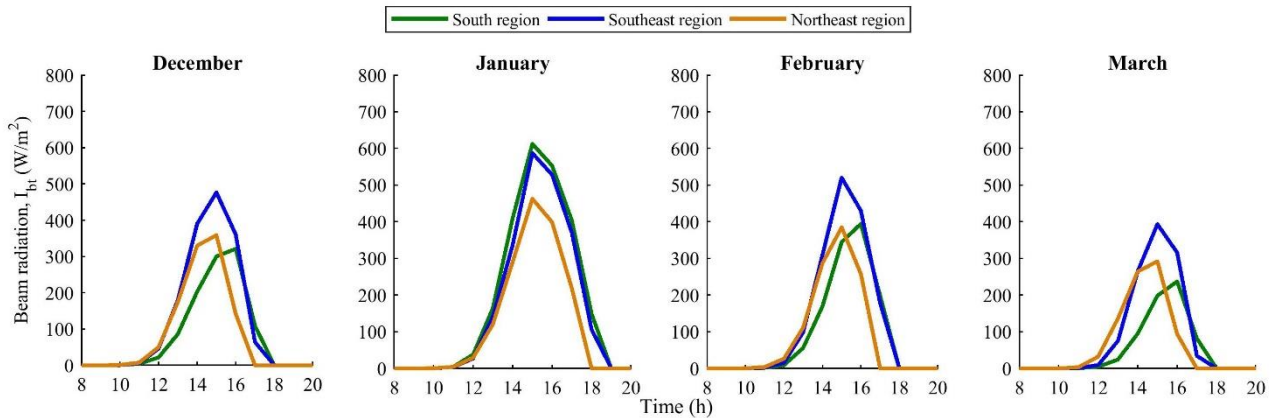


Figure 4 – Direct radiation in the solar concentrator dish.

The production of the shaft power of the Stirling engine is shown in Fig. 5, observing the month of January with greater use in solar energy using a parabolic concentrating dish and Stirling engine. As shown for direct radiation in the concentrating dish, the power of the axis is proportional to this magnitude, so the southeast region is a region that presents a strategic location for the use of this technology.

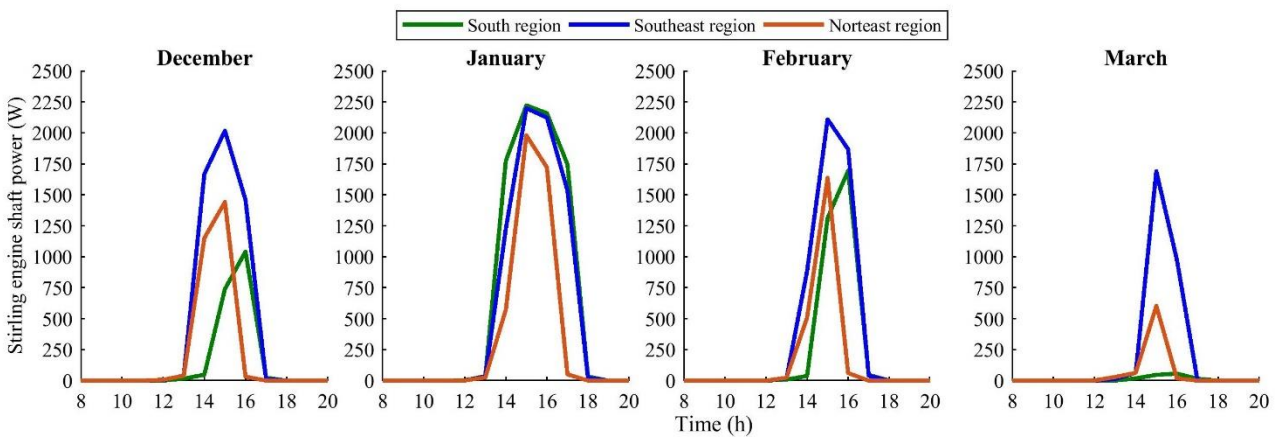


Figure 5 – Stirling engine shaft power.

In the evaluation of each solar station, Table 4. Shows the peak of direct solar radiation in the plane of the parabolic dish and the value of power generation of the Stirling motor shaft. It is observed that the lowest value is found for the São Luiz station with a value of 302 W/m^2 and 776 W , respectively. The other locations, on the other hand, show peaks of Stirling motor shaft output with values above 2000 W . It can be analyzed that the three regions have, as is known in the literature, the capacity of incidence of optimal solar radiation for the use of technology that transforms solar energy into mechanical power, which may be the use of solar concentrating discs and Stirling engines.

Table 4 -Power produced by Stirling engine.

ZONE	CODE	ESTATION	Peak of I_{BT} , W/m ²	Power Stirling, W
Northeast	NAT	Natal	487	2043
	PTR	Petrolina	694	2274
	SLZ	São Luiz	302	776
Southeast	CPA	Cachoeira Paulista	557	2164
	ORN	Ourinhos	503	2079
South	JOI	Joinville	603	2214
	SBR	Sombrio	389	1662
	SMS	São Martinho da Serra	672	2264

5. CONCLUSIONS

The performance of a parabolic concentrating dish system with a Stirling engine was evaluated by combining the modified Iwamoto mathematical model, the solar forecast model, and experimental data measured by solar stations in three Brazilian regions.

The analysis of the solar data allowed, through the global radiation per minute in December, January, February, and March, to determine the average global monthly radiation for eight stations. The experimental database allowed to characterize the behavior of the Northeast, Southeast, and South regions, demonstrating that the average global radiation in the horizontal in Brazil reaches, for these three regions, values above 600 W/m². The production of shaft power, which in the future can be used to generate electricity, reaches values of up to 2121 W. The solar forecast model allowed quantifying the direct radiation in the parabolic concentrating dish, values above 500 W/m² showed that allow the use of concentrating dish technology with power generation through Stirling engine beams.

6. REFERENCES

- Cruz, T., Schaeffer, R., Lucena, A.F.P., Melo, S. and Dutra, R., 2020. Solar water heating technical-economic potential in the household sector in Brazil. *Renewable Energy*, [online] 146, pp.1618–1639.
- Devabhaktuni, V., Alam, M., Shekara Sreenadh Reddy Depuru, S., Green, R.C., Nims, D. and Near, C., 2013. Solar energy: Trends and enabling technologies. *Renewable and Sustainable Energy Reviews*, 19, pp.555–564.
- Duffie, J.A. and Beckman, W.A., 2013. *Solar engineering of thermal processes*. Wiley.
- Mendoza, L.S., Carrillo, G.E., Melian, V.R., and Martinez, A.M., 2017. Mathematical modeling of the geometrical sizing and thermal performance of a Dish/Stirling system for power generation. *Renewable Energy*, 107, pp.23–35.
- Do Nascimento, L.R., Braga, M., Campos, R.A., Naspolini, H.F. and Rüther, R., 2020. Performance assessment of solar photovoltaic technologies under different climatic conditions in Brazil. *Renewable Energy*, [online] 146, pp.1070–1082.
- Prinsloo, G., Dobson, R. and Mammoli, A., 2016. Model based design of a novel Stirling solar micro-cogeneration system with performance and fuel transition analysis for rural African locations. *Solar Energy*, 133, pp.315–330.
- Sandoval, O., Koury, R. and Maia, A., 2016. Design, fabrication and experimental study of a flat plate collector simulator. *Engenharia Térmica*, 15(1), pp.50–56.
- Sandoval, O.R., Caetano, B.C., Borges, M.U., García, J.J. and Valle, R.M., 2019. Modelling and thermal analysis of a solar dish/Stirling system: A case study in Natal, Brazil. *Energy Conversion and Management*, 181, pp.189–201.
- Sripakagorn, A. and Srikam, C., 2011. Design and performance of a moderate temperature difference Stirling engine. *Renewable Energy*, [online] 36(6), pp.1728–1733.
- Xavier, G., Filho, D., Martins, J., Monteiro, P. and Diniz, A., 2015. Simulation of Distributed Generation with Photovoltaic Microgrids—Case Study in Brazil. *Energies*, [online] 8(5), pp.4003–4023.

7. RESPONSIBILITY NOTICE

The authors are the only responsible for the printed material included in this paper.